



Published in final edited form as:

*J Photochem Photobiol B*. 2016 November ; 164: 96–102. doi:10.1016/j.jphotobiol.2016.09.017.

## Low-Level Laser Therapy (904nm) Can Increase Collagen and Reduce Oxidative and Nitrosative Stress in Diabetic Wounded Mouse Skin

José Carlos Tatmatsu Rocha, MsC<sup>\*,1,2,5</sup>, Cleber Ferraresi, PhD<sup>1,5,6</sup>, Michael R. Hamblin, PhD<sup>5</sup>, Flávio Maia Damasceno, PhD<sup>3</sup>, Nilberto Robson Falcão do Nascimento, PhD<sup>4</sup>, Patricia Driusso, PhD<sup>1</sup>, and Nivaldo Antonio Parizotto, PhD<sup>1</sup>

<sup>1</sup>Physical Therapy Department, Federal University of Sao Carlos, Sao Carlos, SP, Brazil

<sup>2</sup>Physical Therapy Department, Federal University of Ceara, Fortaleza, Ce, Brazil

<sup>3</sup>Pharmacology Department, Federal University of Ceara, Fortaleza, CE, Brazil

<sup>4</sup>Ceara State University, Superior Institute of Biomedicine, Laboratory of Renal and Cardiovascular Pharmacology, Fortaleza, Ceará, Brazil

<sup>5</sup>Department of Dermatology, Harvard Medical School, Boston, MA, USA

<sup>6</sup>Wellman Center for Photomedicine, Massachusetts General Hospital, Boston, MA, USA

### Abstract

**Background and Objective**—Over the last decade we have seen an increased interest in the use of Low-Level Laser Therapy (LLLT) in diseases that involve increased oxidative stress. It is well established that hyperglycemia in diabetes elicits a rise in reactive oxygen species (ROS) production but the effect of LLLT remains unclear. This study aimed to investigate whether LLLT was able to improve oxidative/nitrosative stress parameters in the wound healing process in diabetic mice.

**Study Design/Materials and Methods**—Twenty male mice were divided into four groups: non-irradiated control (NIC), irradiated control (IC), non-irradiated and diabetic (NID), irradiated and diabetic (ID). Diabetes was induced by administration of streptozotocin. Wounds were created 120 days after the induction of diabetes in groups IC and ID and these groups were irradiated daily for 5 days (superpulsed 904 nm laser, average power 40 mW, 60 sec). All animals were sacrificed 1 day after the last irradiation and histology, collagen amount, catalase activity, nitrite and thiobarbituric acid reactive substances (TBARS) were measured.

\*Corresponding Author José Carlos Tatmatsu Rocha. 304 Tappan Street Brookline - MA- 02445. Phone: +18572850929. tatmatsu@gmail.com.

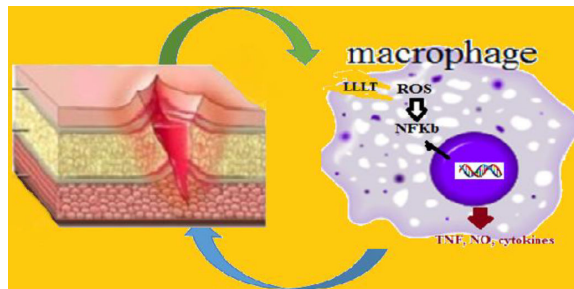
**Publisher's Disclaimer:** This is a PDF file of an unedited manuscript that has been accepted for publication. As a service to our customers we are providing this early version of the manuscript. The manuscript will undergo copyediting, typesetting, and review of the resulting proof before it is published in its final form. Please note that during the production process errors may be discovered which could affect the content, and all legal disclaimers that apply to the journal pertain.

**6.0 CONFLICTS OF INTEREST** The authors declare no conflicts of interest in this research.

**Results**—Histology showed that collagen fibers were more organized in IC and ID when compared to NID group, and significant differences in collagen content were found in group ID versus NID. Catalase activity was higher in IC group compared to other groups ( $p < 0.001$ ). TBARS levels were higher in IC versus NIC, but were lower in ID versus NID ( $p < 0.001$ ). Nitrite was lower in both irradiated groups versus the respective non-irradiated groups ( $p < 0.001$ ).

**Conclusions**—Delayed wound healing in diabetes is still a challenge in clinical practice with high social costs. The increased production of collagen and decreased oxidative and nitrosative stress suggests that LLLT may be a viable therapeutic alternative in diabetic wound healing.

### Graphical abstract



LLL is an alternative treatment for use in diabetic wounds that can improve tissue oxidative profile. In this study, we used LLLT 904 nm in mouse diabetic induced to investigate the effects of lasertherapy on oxidative stress. We believe that LLLT not only enhances mitochondrial respiration, but also activates the redox-sensitive NFkB signaling via generation of ROS. NF-kappaB regulates immune and inflammatory responses in macrophages as well as production of inflammatory cytokines like TNF-alpha and NO through iNOS expression.

### Keywords

catalase; diabetes mellitus; oxidative stress; collagen production; nitric oxide; TBARS; photobiomodulation

## 1.0 INTRODUCTION

Diabetes mellitus (DM) is characterized by elevated blood glucose levels, an impaired blood supply, and increased production of reactive oxygen species (ROS) [1]. Chronic ROS generation is implicated in the pathogenesis of many illnesses, including atherosclerosis and inflammation [2, 3]. The hyperglycemia caused by diabetes elicits an increase in ROS production, due to overproduction of superoxide by the mitochondrial electron-transport chain [4]. In addition to this oxidative stress, the inflammatory response induced by epidermal injury in wounds provokes the migration and accumulation of neutrophils and macrophages, which also produce ROS via their respiratory burst. When there is increased production of ROS coupled with decreased antioxidant defenses, oxidative stress occurs, and the ROS interacts with cellular molecules and enhances the process of lipid peroxidation (LPO), causing DNA damage and/or inducing protein and nucleic acid turnover [5].

Furthermore, macrophages release nitric oxide (NO) via activated inducible nitric oxide synthase (iNOS) [6]. However, the synthesis of large amounts of NO can produce nitrosative stress by reacting with superoxide to form peroxynitrite. Many authors have proposed that low level-laser therapy (LLLT) is able to influence oxidative stress parameters as well as to change the activity of antioxidant enzymes and the production of ROS [1]. Over the last decade the literature has been reported an increased interest in the application of photobiomodulation using different light sources in diseases related to increased oxidative stress, but the mechanisms involved in this response remain unclear, especially in relation to the effects of LLLT on the mitochondrial respiratory chain and on biomarkers of oxidative stress. The basic biological mechanism behind the effects of LLLT is thought to be via absorption of red and infra red light by cytochrome c oxidase (complex IV of the mitochondrial respiratory chain) [7]. In addition, Karu [8] and other authors [9] have proposed that one of the possible mechanisms of action of LLLT, is a brief and modest increase in production of ROS such as superoxide ( $O_2^-$ ) and hydrogen peroxide ( $H_2O_2$ ), leading to restoration of the redox imbalance as a consequence of enhanced production of antioxidant enzymes. LLLT alters the redox state in cells and can induce the activation of intracellular signaling, increase activation of redox-sensitive transcription factors [10], and affect enzyme activation and cell cycle progression [7] which are fundamental mechanisms involved in wound healing. Several parameters are important for optimizing treatment using photobiomodulation. These parameters include wavelength, power density, energy, time, and frequency of application. The goal of this study was to test if near-infrared laser (904 nm) could modulate oxidative/nitrosative stress responses in diabetic wounded mouse skin.

## 2.0 MATERIALS AND METHODS

### 2.1 Animals

CEPA/UFC (IACUC) approved the study under protocol number 01/2013. All experiments were performed in accordance with the National Institutes of Health Guide for Care and Use of Laboratory Animals. The animals used were bred in the Department of Pathology, Faculty of Medicine, Federal University of Ceara and kept in an environment with a constant temperature of 24°C and light/dark cycle of 12 hours. We used 20 male Swiss mice, weighing 25–30 g at baseline. The animals were randomly allocated into four groups: non-irradiated control (NIC), irradiated control (IC), non-irradiated and diabetic (NID) and irradiated diabetic (ID). Ten animals were induced into a diabetic state by administration of streptozotocin and 10 animals remained euglycemic (control).

### 2.2 Diabetes induction

For induction of diabetes we used a previously described methodology [11]. The mice were subjected to fasting for 6 hours and then anesthetized by thiopental (40mg/kg/2.5% IP) and kept in a prone position for an intraperitoneal (IP) injection of streptozotocin (solution 70mg/kg - STZ) dissolved in citrate buffer solution (pH 4.5). Six hours after administration, the animals had their water supply replaced by an aqueous solution of glucose (10%) for 24 hours. Glucose levels were determined in blood samples taken from the tail vein and measured on a glucose meter (*AccuChek*, Roche Diagnostics, Indianapolis, IN).

### 2.3 Wound creation

The animals were anesthetized by intraperitoneal injection of thiopental. Each animal was placed in a prone position, without immobilization, in order to shave the dorsal region with a razor and soap. The skin of the animal was cleaned with an antiseptic solution of 2% chlorhexidine and it was cut with a carbon steel surgical blade until the depth reached the hypodermis. In order to standardize the lesions, we used a surgical field with 2 cm width and 2 cm long, with reference to the animal's posterior iliac crest, which was labeled with an alcohol soluble marker (see figure 1).

### 2.4 Low-level laser therapy (LLLT)

The wounds were irradiated at a single point over the incision with laser device: Laserpulse (IBRAMED, Amparo, Brazil), class 3B, superpulsed 904 nm GaAs diode laser with parameters according to Table 1. The laser treatment was repeated daily for 5 consecutive days. The animals in groups IC and ID received laser irradiation with the probe perpendicular to the wound. Other groups received contact with the probe laser off and the lesions were then treated with saline 0.9% NaCl. Wood chip bedding in the cages were not used due to the risk of infection/contamination, and cages were cleaned daily. One day after the last irradiation, the animals were euthanized by decapitation to remove the skin lesion for homogenization and subsequent analysis.

### 2.5 Histopathological analysis

The skin samples were fixed in 10 % buffered formalin (Merck, Darmstadt, Germany) for 24 h. Afterwards, they were dehydrated and embedded in paraffin blocks. Three sections (5 $\mu$ m) from each specimen were longitudinally sectioned (Microtome Leica Microsystems SP 1600, Nussloch, Germany) and stained with hematoxylin and eosin (H.E. stain, Merck, Darmstadt, Germany). The morphological description of the healing characteristics was performed with optical microscopy (Olympus Optical Co., Tokyo, Japan) and histological analysis was made by a pathologist in a double-blind manner. Five slides from each specimen were analyzed and the following criteria were scored as absent, discrete, moderate or intense: granulation tissue, inflammatory process, area of fibrosis and fibroblast number.

### 2.6 Collagen Analysis by Masson Staining

Sections stained with Masson were examined microscopically and the images used for analysis were captured by microscopy using a 20X objective (Carl Zeiss, Germany) and a capture system consisting of a camera (Olympus Optical Co., Tokyo, Japan) equipped with AxioVision 4.7.2.0 software. The processing and image analysis were performed with the public domain software ImageJ 1.36 version (National Institutes of Health, Bethesda, USA; <http://rsbweb.nih.gov/ij/>) using plugin *color deconvolution* and the values of the amount of collagen as described in previous studies [12–14].

### 2.7 Procedure for determination of the antioxidant activity

The skin was immediately dissected and homogenized in 1.15% KCl, volume equivalent to 10 times its weight (1g/10 ml solution). The mixture was centrifuged (5,800 rpm, 10 min at

10°C), and the supernatant was used for biochemical determinations (TBARS, catalase activity and nitrite) according to Figure 2:

**2.7.1 Concentration of thiobarbituric acid reactive substances (TBARS)**—Lipid peroxidation was assessed by measuring the concentration of thiobarbituric acid reactive substances (TBARS). In this process, two molecules of thiobarbituric acid react with a molecule of malondialdehyde to form a pink pigment with maximum absorbance in acid solution at 532–535 nm. TBARS was determined in the skin homogenates that had been diluted to 10% (w/v). Then, 250 µL of homogenate were incubated in a water bath at 37°C for 1 hour, followed by addition of 400 µL of 35% perchloric acid to precipitate the protein. The mixture was centrifuged at 14,000 rpm at 4 °C for 10 minutes and then the supernatant was added to 200 µL of 1.2% thiobarbituric acid. Next, the mixture was again incubated in a water bath at 100°C for 30 minutes. After cooling on ice, samples were read in a spectrophotometer at 535 nm.

**2.7.2 Determination of catalase activity**—The skin of mice was homogenized in a 0.1 M sodium phosphate buffer solution, pH 7.0, at an equivalent volume of 200 times its weight. Then, the homogenate was centrifuged at 5,800 rpm, 10 min at 4°C, the upper layer was discarded and the bottom layer was used for spectrophotometric measurements of H<sub>2</sub>O<sub>2</sub> at 230 nm (28). In the cuvette, were added 980 µL of the reaction medium (15% H<sub>2</sub>O<sub>2</sub>, in 1 M Tris-HCL buffer), containing 5 mM EDTA, pH 8.0, and 20 µL of the sample diluted in the Tris-HCl buffer. Initial and final absorbance was recorded at 230 nm, after 1 and 6 min, respectively. A standard curve was established using purified catalase (Sigma, MO, USA). Results were expressed in mmol/min/mg protein. Protein was determined by the Lowry method.

**2.7.3 Nitrite concentration**—Nitrite concentration was measured from homogenates of the mice skin. Homogenates of the treated and control groups were diluted to 10% (w/V) in 50 mM phosphate buffer, pH 7.4 and centrifuged at 14,000 rpm for 15 minutes at 4 °C. The concentration of nitrite was determined by a diazotization chromophore reaction that forms a pinkish color with a peak absorbance of 560 nm. 250 µL of the Griess reagent (1% sulfanilamide, N-(1-naphthyl)-ethylenediamine 0.1%, 1.0% phosphoric acid and distilled water in the ratio of 1:1:1:1) were added to 250 µL of homogenate (supernatant) and the mixture was maintained at room temperature for 10 minutes. Thereafter, the absorbance of the samples was determined by spectrophotometry at 560 nm and the blank prepared by adding 250 µL of the Griess reagent to 250 µL of 50 mM phosphate buffer, pH 7.4. The absorbance values were interpolated on a calibration curve containing NaNO<sub>2</sub> concentrations ranging from 0.75 to 100 µM.

## 2.8 Statistical Analysis

Data were expressed as mean and standard deviation and statistically analyzed by analysis of variance (ANOVA) one-way with Bonferroni post hoc test. The significance level was set at  $p < 0.05$ . We used the statistical software package SPSS, version 18.0.

## 3.0 RESULTS

### 3.1 Histopathological analysis

Representative histological sections of the four groups are shown in Fig. 3.I and 3.II. Five days post wounding, the NIC and IC groups (Figure 3A and 3B respectively) showed a discrete inflammatory infiltrate, with partial healing and a moderate amount of granulation tissue that was rich in newly formed blood vessels and fusiform fibroblasts. Masson staining showed a moderate deposition of a disorganized mature collagen matrix in the NIC group and a more organized and more intense degree of collagen deposition in the IC group (Figure 3E and 3F respectively). A moderate inflammatory infiltrate, a modest amount of fibroblasts and a granulation tissue that was poor in newly formed blood vessels was observed in the NID group (Figure 3C). On the other hand a moderate amount of fusiform fibroblasts and an increased density of blood vessels was observed in the ID group (Figure 3C). Masson red staining showed an intense deposition of a more organized collagen matrix in the ID group (Figure 3H) when compared with the NID group (Figure 3G).

### 3.2 Collagen amount

The images were analyzed taking into account differences between thin and thick fibers and the relative percentage of collagen in the examined fields. The data showed significant differences between NIC versus ID groups with regard to red stained fibers (type I fibers) ( $p < 0.01$ ) and between the ID group versus NIC and NID groups (type II fibers) ( $p < 0.03$ ) (table 2).

### 3.3 Concentration of TBARS

As seen in Table 3, the average concentration of TBARS in the four groups was significantly different ( $F = 12.888$ ,  $P = 0.001$ ). The Bonferroni test showed significant differences between the groups: ID had a decreased concentration of TBARS compared to NID ( $p < 0.05$ ) and IC had an increased concentration of TBARS compared to NIC ( $p < 0.05$ ). In addition, group ID showed significantly lower levels of TBARS than group IC ( $p < 0.05$ ).

### 3.4 Catalase activity

As seen in Figure 4, the levels of catalase in the four groups were significantly different ( $p = 0.001$ ). An increase in catalase activity was observed for IC mice, when their results were compared with those obtained from NIC and ID mice. The Bonferroni test (post hoc) showed that group IC had higher catalase activity compared to NIC group ( $p = 0.05$ ). Other comparisons between groups were not statistically different ( $p > 0.05$ ).

### 3.5 Nitrite concentration

As seen in Figure 5, the concentration of nitrite in the four groups was significantly different ( $F = 54.128$ ,  $p = 0.001$ ). The Bonferroni test showed a decreased concentration of nitrite in group ID compared to group NID ( $p < 0.05$ ), and group IC had decreased nitrite concentration compared to group NIC ( $p < 0.05$ ). There was no significant difference between groups ID and IC ( $p > 0.05$ ).

## 4.0 DISCUSSION

Diabetes mellitus (DM) is an endocrine metabolic disease whose main clinical manifestation is hyperglycemia, which promotes oxidative stress due increased production of mitochondrial ROS and increased non-enzymatic glycosylation of proteins, as well as via the activation of several cellular transcription factors [4]. It is well known that one of the main pathological abnormalities that are suffered by diabetic patients, is caused by difficulties in wound healing [15, 16], and new approaches are needed to accelerate tissue repair in diabetic patients [17–19].

Photobiomodulation or LLLT has been studied extensively in several models of wound healing, and most previous reports have found beneficial effects for this modality of treatment. However, only a few studies have investigated the relationship between LLLT and its effects on oxidative and nitrosative stress in the wounded skin of chronic diabetic mice [20]. Hyperglycemia-induced oxidative stress may cause tissue damage and induces hydroxyl radical generation that is correlated with the level of thiobarbituric acid (TBARS) reactive compounds used as an estimation of lipid peroxidation [21, 22]. Based on these facts, our hypothesis was that LLLT could reduce nitrosative/oxidative stress parameters in diabetic mice and thus accelerate the tissue repair process. However, it is important to emphasize that the effects of LLLT could depend on the total energy, power density, timing and frequency of irradiation, and the wavelength and other characteristics of the laser or light source used [7]. Therefore, the present manuscript used the same wavelength (904 nm) and similar energy per point (2.39 J) previously reported (904 nm, 2.34 J) [23] as beneficial to wound healing in rats. Moreover, the average power of the light (39.9 mW) used in the present study was thought to be low due to the target tissue treated (skin), which is superficial and does not require a deep light penetration.

Oxidation is a normal part of aerobic metabolism and ROS are produced naturally at a certain level, but at greatly elevated levels as a result of some pathological disease states. Antioxidants are substances that fight ROS and free radicals, and can act enzymatically, such as glutathione peroxidase, catalase and superoxide dismutase, or can act non-enzymatically for example: ascorbate, vitamin E, histidine peptides, and some iron-sequestering proteins (ferritin and transferrin). Inflammatory processes can generate ROS and reactive nitrogen species (RNS). The RNS include nitric oxide (NO•) in large amounts, and peroxynitrite (ONOO-). The presence of nitric oxide in biological systems promotes RNS production such as peroxynitrite (formed by spontaneous reaction between NO and superoxide) that reacts with tyrosine residues in proteins to form nitrotyrosine[24]. Besides, nitrites and nitrates that circulate in the blood are produced from NO oxidation.

Photobiomodulation can produce NO through photodissociation of NO that is bound to cytochrome c oxidase (CCO). CCO is a photoacceptor located in the inner mitochondrial membrane whose function is to catalyze the oxidation of cytochrome c and the reduction O<sub>2</sub> to water, resulting in the pumping of protons out of the mitochondrial matrix. CCO has two heme centers (aa and a3) and two copper centers (CuA and CuB), of which the heme iron of cytochrome a3 and CuB together forms the O<sub>2</sub> binding site [25]. Thus, NO may compete with oxygen to bind to the iron-sulfur complex and to the iron and copper centers in the

respiratory chain and inhibit the mitochondrial ATP (adenosine tri-phosphate) synthesis [26]. It is proposed that the NO-CCO bond can be broken by visible and NIR photon absorption [27] to restore mitochondrial function and increase ATP synthesis [27, 28]. Our results showed a significant reduction of nitrite levels by LLLT in the skin homogenate of wounded mice (Figure 5). This could be explained due to a possible protective effect that LLLT could have on the microvasculature because some studies [29] have suggested that hyperglycemia is a factor which naturally leads to injury of blood vessels and causes long-term microvascular and macrovascular complications. The excessive production of NO may also lead to endothelial injury. Volpe et al demonstrated that the hyperglycemia typical of diabetes exacerbated *in vitro* inflammatory responses [30]. Their group observed that levels of NO, interleukin-6 (IL-6), tumor necrosis factor alpha (TNF-alpha), and malondialdehyde (MDA) were higher in supernatant of blood cells that had been stimulated with palmitate. Advanced studies have suggested that the effects of hyperglycemia and hyperlipidemia on peripheral blood mononuclear cells (PBMNC) include activation of the nicotinamide adenine dinucleotide phosphate (NADPH) oxidase system leading to ROS production, enhanced nuclear factor kappa-light-chain-enhancer of activated B cells (NF-kB) activity, and increased levels of cytokines, chemokines, and circulating adhesion molecules [31–33]. We believe that one important factor to explain our results may be mediated by NFkB, because a previous report [10] suggested that LLLT not only enhanced mitochondrial respiration, but also activated the redox-sensitive NF-kB transcription factor via brief generation of ROS. NF-kB regulates immune and inflammatory responses in endothelial cells, vascular smooth muscle cells, and macrophages [34] as well as production of inflammatory cytokines, TNF-alpha and NO (through inducible isoform of nitric oxide synthase expression - iNOS) [35]. Our findings agree with Kandolf-Sekulovic *et al* [20] who used LLLT (904 nm, irradiance 60 mW/cm<sup>2</sup>, fluence 3.6 J/ cm<sup>2</sup>) in a model of contact hypersensitivity (CHS in albino Oxford rats) and observed a reduced release of nitric oxide by the inflammatory cells. These authors suggested that lower levels of NO were caused by fewer inflammatory cells in the dermis, and a possible lower capacity for NO production by skin resident cells (keratinocytes and Langerhans cells). These cells have been suggested to be the NO-producing cells in the CHS skin reaction [36]. Eduardo et al [37] analyzed peroxynitrite formation in zymosan-induced arthritis in rats, and found inhibition of joint hyperalgesia that correlated with decreased nitric oxide levels and nitrotyrosine levels in the joint exudates, when compared to control rats. Taken together, these results point towards a homeostatic role of low levels of NO derived from the constitutive NOS enzymes. Moreover other studies utilizing different experimental models have suggested that LLLT is able to induce SOD expression, decreasing the available concentration of superoxide anion and, as a result, reduce peroxynitrite production [20].

We found that catalase activity was increased significantly between groups IC versus NIC and ID. The suppression of catalase activity in diabetic animals is known to be involved in the susceptibility of diabetics to ROS [38]. In addition, a certain level of oxidative stress is known to be required for the satisfactory induction of neovascularization in response to ischemia and tissue damage [39]. A further possible mechanism to explain these results is that high glucose levels have been associated with low neutrophil chemotactic activity [40, 41] and reduction of the phagocytic activity of polymorphonuclear cells in diabetic patients



[42, 43]. Chamon et al[44] showed a 370% and 199% increase in ROS generation during the process of phagocytosis in healthy subjects and DM patients respectively. In the presence of pyruvate, these percentage increases were reduced to 81% and 80%, respectively. Therefore pyruvate exhibited a suppressive action on granulocytes both in healthy individuals and DM patients. One effect of LLLT could be on pyruvate levels associated with a metabolic signaling pathway depending on the oxidizing profile of the target cell. Pyruvate is associated with protection of different cells against oxidative damage through non-enzymatic scavenging of ROS including  $H_2O_2$  [45]. Therefore, pyruvate could selectively cause reduction of  $H_2O_2$  to prevent the generation of the hydroxyl radical ( $OH\bullet$ ). On the other hand, Karu [46] reported that laser photobiomodulation decreased production of superoxide anion and also increased catalase activity (antioxidant), leading to an increased protein synthesis in a culture of yeast cells.

An important factor to consider is that during oxidative stress, membrane lipids are continuously subjected to lipid peroxidation, shown by an increase in TBARS. In diabetes, lipid peroxidation is a possible factor that influences insulin resistance. Previous studies [38] found high TBARS levels in the blood and in the lung tissue in diabetes mellitus, suggesting that lipid peroxidation occurred in the first 60 days after onset of the disease. In this context, Silveira et al.[28] demonstrated a significant reduction of lipid peroxidation in rats treated with 2 J/cm<sup>2</sup> and 4 J/cm<sup>2</sup>, suggesting that LLLT stimulated antioxidant mechanisms that protected against oxidative damage in lipid membranes. In our study, LLLT significantly reduced the amount of MDA generated in the skin of the mice (Table. 2). Many studies in experimental models have shown that LLLT can modulate ROS/RNS by lowering lipid peroxidation (TBARS and MDA) [47, 48] and reducing RNS by inhibiting synthesis of iNOS [48], and increasing the activity of respiratory [38] chain for increased ATP synthesis.

## 5.0 CONCLUSIONS

In this work our findings in the wounds of diabetic animals indicated a possible protective effect that 904 nm laser could have on the microvasculature, with lowered levels of nitrite, and increased protection against oxidative damage in lipid membranes. Besides, the better-organized and increased amount of collagen fibers demonstrated that LLLT could be effective in clinical practice with poorly healing diabetic wounds. The beneficial antioxidant effects observed in diabetic animals opens the possibility of using LLLT as a treatment for wounds such as diabetic foot ulcers, and other disorders resulting from diabetes mellitus.

## Acknowledgments

**FUNDING SOURCES** JCTR was supported by CAPES / PDSE (Coordenação de Aperfeiçoamento de Pessoal-Process no. 006648/2015-00). CF was supported by Fundação de Amparo a Pesquisa do Estado de São Paulo (FAPESP-Process no. 2010/07194-7) in Brazil. MRH was supported by US NIH (grant R01AI050875). The authors express their thanks to professors Walberto dos Santos and Tatiana Sato and to the Laboratory of Pharmacology, Federal University of Ceara for all support with chemical reagents.

## 7.0 REFERENCES

- [1]. Santos N, dos Santos J, dos Reis J, Oliveira P, de Sousa A, Carvalho C, Soares L, Marques A, Pinheiro A. Influence of the use of laser phototherapy ( $\lambda$ 660 or 790 nm) on the survival of

cutaneous flaps on diabetic rats. *Photomedicine and laser surgery*. 2010;483–488. [PubMed: 19831497]

- [2]. Ames BN, Shigenaga MK, Hagen TM. Oxidants, Antioxidants, And the Degenerative Diseases of Aging. *Proceedings of the National Academy of Sciences of the United States of America*. 1993; 90:7915–7922. [PubMed: 8367443]
- [3]. Wiseman H, Halliwell B. Damage to DNA by reactive oxygen and nitrogen species: Role in inflammatory disease and progression to cancer. *Biochemical Journal*. 1996; 313:17–29. [PubMed: 8546679]
- [4]. Brownlee M. Biochemistry and molecular cell biology of diabetic complications. *Nature*. 2001; 414:813–820. [PubMed: 11742414]
- [5]. Dean RT, Fu SL, Stocker R, Davies MJ. Biochemistry and pathology of radical-mediated protein oxidation. *Biochemical Journal*. 1997; 324:1–18. [PubMed: 9164834]
- [6]. Stocker R, Keaney JF Jr. Role of oxidative modifications in atherosclerosis. *Physiol Rev*. 2004; 84:1381–1478. [PubMed: 15383655]
- [7]. Gupta A, Avci P, Sadasivam M, Chandran R, Parizotto N, Vecchio D, de Melo WC, Dai T, Chiang LY, Hamblin MR. Shining light on nanotechnology to help repair and regeneration. *Biotechnology advances*. 2012
- [8]. Karu T. Primary and secondary mechanisms of action of visible to near-IR radiation on cells. *J Photochem Photobiol B*. 1999; 49:1–17. [PubMed: 10365442]
- [9]. Chen AC-H, Huang Y-Y, Arany PR, Hamblin MR. Role of reactive oxygen species in low level light therapy. *Proc SPIE*. 2009; 7165 doi: 10.1117/1112.814890.
- [10]. Chen AC, Arany PR, Huang YY, Tomkinson EM, Sharma SK, Kharkwal GB, Saleem T, Mooney D, Yull FE, Blackwell TS, Hamblin MR. Low-level laser therapy activates NF- $\kappa$ B via generation of reactive oxygen species in mouse embryonic fibroblasts. *PLoS One*. 2011; 6:e22453. [PubMed: 21814580]
- [11]. Farias VX, Macedo FH, Oquendo MB, Tome AR, Bao SN, Cintra DO, Santos CF, Albuquerque AA, Heimark DB, Lerner J, Fonteles MC, Leal-Cardoso JH, Nascimento NR. Chronic treatment with D-chiro-inositol prevents autonomic and somatic neuropathy in STZ-induced diabetic mice. *Diabetes Obes Metab*. 2011; 13:243–250. [PubMed: 21205116]
- [12]. Collins TJ. ImageJ for microscopy. *Biotechniques*. 2007; 43:25.
- [13]. Smolle J. Computer recognition of skin structures using discriminant and cluster analysis. *Skin Research and Technology*. 2000; 6:58–63. [PubMed: 11428943]
- [14]. Miot HA, Brianezi G. Morphometric analysis of dermal collagen by color clusters segmentation. *Anais Brasileiros De Dermatologia*. 2010; 85:361–364. [PubMed: 20676470]
- [15]. Francis-Goforth KN, Harken AH, Saba JD. Normalization of diabetic wound healing. *Surgery*. 2010; 147:446–449. [PubMed: 19703697]
- [16]. Adams SB Jr, Sabesan VJ, Easley ME. Wound healing agents. *Foot Ankle Clin*. 2006; 11:745–751. [PubMed: 17097514]
- [17]. Demidova-Rice TN, Hamblin MR, Herman IM. Acute and Impaired Wound Healing: Pathophysiology and Current Methods for Drug Delivery, Part 2: Role of Growth Factors in Normal and Pathological Wound Healing: Therapeutic Potential and Methods of Delivery. *Adv Skin Wound Care*. 2012; 25:349–370. [PubMed: 22820962]
- [18]. Demidova-Rice TN, Hamblin MR, Herman IM. Acute and Impaired Wound Healing: Pathophysiology and Current Methods for Drug Delivery, Part 1: Normal and Chronic Wounds: Biology, Causes, and Approaches to Care. *Adv Skin Wound Care*. 2012; 25:304–314. [PubMed: 22713781]
- [19]. Tatmatsu Rocha JC, Jansem de Almeida Catanho MT, da Mota DL. Application of the Laser Radiation in Patients of Pressure Ulcers: Clinical and Histomorphometric Analysis of the Derm. *Brazilian Archives of Biology and Technology*. 2008; 51:231–234.
- [20]. Kandolf-Sekulovic L, Kataranovski M, Pavlovic MD. Immunomodulatory effects of low-intensity near-infrared laser irradiation on contact hypersensitivity reaction. *Photodermatology Photoimmunology & Photomedicine*. 2003; 19:203–212.
- [21]. Ohkuwa T, Sato Y, Naoi M. Hydroxyl Radical Formation in Diabetic Rats Induced by Streptozotocin. *Life Sciences*. 1995; 57:1325–1325.

- [22]. Winiarska K, Drozak J, Wegrzynowicz M, Fraczyk T, Bryla J. Diabetes-induced changes in glucose synthesis, intracellular glutathione status and hydroxyl free radical generation in rabbit kidney-cortex tubules. *Molecular and Cellular Biochemistry*. 2004; 261:91–98. [PubMed: 15362490]
- [23]. Sanati MH, Torkaman G, Hedayati M, Dizaji MM. Effect of Ga-As (904nm) and He-Ne (632.8 nm) laser on injury potential of skin full-thickness wound. *J Photochem Photobiol B*. 2011; 103:180–185. [PubMed: 21450490]
- [24]. Pacher P, Liaudet L, Soriano FG, Mabley JG, Szabo E, Szabo C. The role of poly(ADP-ribose) polymerase activation in the development of myocardial and endothelial dysfunction in diabetes. *Diabetes*. 2002; 51:514–521. [PubMed: 11812763]
- [25]. Ferraresi, C.; Hamblin Mr Fau - Parizotto, NA.; Parizotto, NA. Low-level laser (light) therapy (LLLT) on muscle tissue: performance, fatigue and repair benefited by the power of light.
- [26]. Huang Y-Y, Sharma SK, Carroll J, Hamblin MR. BIPHASIC DOSE RESPONSE IN LOW LEVEL LIGHT THERAPY - AN UPDATE. *Dose-Response*. 2011; 9:602–618. [PubMed: 22461763]
- [27]. Vladimirov YA, Osipov AN, Klebanov GI. Photobiological principles of therapeutic applications of laser radiation. *Biochemistry-Moscow*. 2004; 69:81–90. [PubMed: 14972023]
- [28]. Silveira PC, Silva LA, Fraga DB, Freitas TP, Streck EL, Pinho R. Evaluation of mitochondrial respiratory chain activity in muscle healing by low-level laser therapy. *J Photochem Photobiol B*. 2009; 95:89–92. [PubMed: 19232497]
- [29]. Bagasra O, Michaels FH, Zheng YM, Bobroski LE, Spitsin SV, Fu ZF, Tawadros R, Koprowski H. Activation of the inducible form of nitric oxide synthase in the brains of patients with multiple sclerosis. *Proceedings of the National Academy of Sciences of the United States of America*. 1995; 92:12041–12045. [PubMed: 8618840]
- [30]. Oliveira Volpe CM, Machado Abreu LF, Gomes PS, Gonzaga RM, Veloso CA, Nogueira-Machado JA. The Production of Nitric Oxide, IL-6, and TNF-Alpha in Palmitate-Stimulated PBMNCs Is Enhanced through Hyperglycemia in Diabetes. *Oxidative Medicine and Cellular Longevity*. 2014
- [31]. Kolb H, Mandrup-Poulsen T. An immune origin of type 2 diabetes? *Diabetologia*. 2005; 48:1677–1677. (vol 48, pg 1038, 2005).
- [32]. Tripathy D, Mohanty P, Dhindsa S, Syed T, Ghanim H, Aljada A, Dandona P. Elevation of free fatty acids induces inflammation and impairs vascular reactivity in healthy subjects. *Diabetes*. 2003; 52:2882–2887. [PubMed: 14633847]
- [33]. Guha M, Bai W, Nadler JL, Natarajan R. Molecular mechanisms of tumor necrosis factor alpha gene expression in monocytic cells via hyperglycemia-induced oxidant stress-dependent and -independent pathways. *Journal of Biological Chemistry*. 2000; 275:17728–17739. [PubMed: 10837498]
- [34]. Sena CM, Pereira AM, Fernandes R, Santos-Silva D, Faustino A, Ceica R. Novel therapeutic approach to target endothelial dysfunction in type 2 diabetes. *Cardiovascular Research*. 2014; 103
- [35]. Suganami T, Tanimoto-Koyama K, Nishida J, Itoh M, Yuan X, Mizuarai S, Kotani H, Yamaoka S, Miyake K, Aoe S, Kamei Y, Ogawa Y. Role of the Toll-like receptor 4/NF-kappa B pathway in saturated fatty acid-induced inflammatory changes in the interaction between adipocytes and macrophages. *Arteriosclerosis Thrombosis and Vascular Biology*. 2007; 27:84–91.
- [36]. Ross R, Gillitzer C, Kleinz R, Schwing J, Kleinert H, Forstermann U, Reske-Kunz AB. Involvement of NO in contact hypersensitivity. *International Immunology*. 1998; 10:61–69. [PubMed: 9488156]
- [37]. Eduardo FP, Mehnert DU, Monezi TA, Zzell DM, Schubert MM, Eduardo CP, Marques MM. Cultured epithelial cells response to phototherapy with low intensity laser. *Lasers Surg Med*. 2007; 39:365–372. [PubMed: 17457843]
- [38]. Dhaunsi GS, Bitar MS. Antioxidants attenuate diabetes-induced activation of peroxisomal functions in the rat kidney. *J Biomed Sci*. 2004; 11:566–570. [PubMed: 15316130]
- [39]. Urbich C, Dernbach E, Aicher A, Zeiher AM, Dimmeler S. CD40 ligand inhibits endothelial cell migration by increasing production of endothelial reactive oxygen species. *Circulation*. 2002; 106:981–986. [PubMed: 12186804]

- [40]. Mowat AG, Baum J. Chemotaxis of Polymorphonuclear Leukocytes from Patients with Diabetes Mellitus. *New England Journal of Medicine*. 1971; 284:621. [PubMed: 5545603]
- [41]. Collison KS, Parhar RS, Saleh SS, Meyer BF, Kwaasi AA, Hammami MM, Schmidt AM, Stern DM, Al-Mohanna FA. RAGE-mediated neutrophil dysfunction is evoked by advanced glycation end products (AGEs). *Journal of Leukocyte Biology*. 2002; 71:433–444. [PubMed: 11867681]
- [42]. Chanchamroen S, Kewcharoenwong C, SUSAENGAT W, ATO M, LERTMEMONGKOLCHAI G. Human Polymorphonuclear Neutrophil Responses to *Burkholderia pseudomallei* in Healthy and Diabetic Subjects. *Infection and Immunity*. 2009; 77:456–463. [PubMed: 18955471]
- [43]. Lin J-C, Siu LK, Fung C-P, Tsou H-H, Wang J-J, Chen C-T, Wang S-C, Chang F-Y. Impaired phagocytosis of capsular serotypes K1 or K2 *Klebsiella pneumoniae* in type 2 diabetes mellitus patients with poor glycemic control. *Journal of Clinical Endocrinology & Metabolism*. 2006; 91:3084–3087. [PubMed: 16720670]
- [44]. Chamon JSF, Fagundes-Netto FS, Gonzaga RM, Gomes PS, Volpe C.M.d.O. Nogueira-Machado JA. Absence of pyruvate anti-oxidant effect on granulocytes stimulated toll-like receptors. *Free Radicals and Antioxidants*. 2013; 3(Supplement):S11–S15.
- [45]. Moriguchi N, Hinoi E, Tsuchihashi Y, Fujimori S, Iemata M, Takarada T, Yoneda Y. Cytoprotection by pyruvate through an anti-oxidative mechanism in cultured rat calvarial osteoblasts. *Histology and Histopathology*. 2006; 21:969–977. [PubMed: 16763947]
- [46]. Karu T, Pyatibrat L, Kolyakov S, Afanasyeva N. Absorption Measurements of Cell Monolayers Relevant to Mechanisms of Laser Phototherapy: Reduction or Oxidation of Cytochrome c Oxidase Under Laser Radiation at 632.8 nm. *Photomedicine and Laser Surgery*. 2008; 26:593–599. [PubMed: 19099388]
- [47]. Luo L, Sun Z, Zhang L, Li X, Dong Y, Liu TC-Y. Effects of low-level laser therapy on ROS homeostasis and expression of IGF-1 and TGF-beta 1 in skeletal muscle during the repair process. *Lasers in Medical Science*. 2013; 28:725–734. [PubMed: 22714676]
- [48]. Rizzi CF, Mauriz JL, Freitas Correa DS, Moreira AJ, Zettler CG, Filippin LI, Marroni NP, Gonzalez-Gallego J. Effects of low-level laser therapy (LLLT) on the nuclear factor (NF)-kappa B signaling pathway in traumatized muscle. *Lasers in Surgery and Medicine*. 2006; 38:704–713. [PubMed: 16799998]

### Highlights

- Hyperglycemia from diabetes causes a rise in reactive oxygen species (ROS) production and inhibits wound healing.
- A diabetic mouse model of cutaneous wounds was treated with superpulsed 904 nm laser therapy (LLLT).
- LLLT increased collagen synthesis, with better-organized fibers, and more formation of new blood vessels.
- LLLT increased catalase, reduced oxidative stress and nitrosative stress in diabetic mouse wounds.
- LLLT could be clinically applied to non-healing diabetic wounds with an additional antioxidant effect



**Figure 1.**  
Wound creation: the skin was cut with a carbon steel surgical blade until it reached the hypodermis with 2 cm width and 2 cm long.

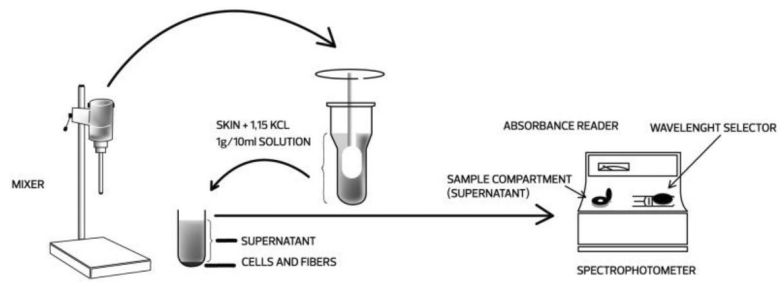


**Figure 2.** Schematic drawing showing procedure for determination of the antioxidant activity. The skin was dissected and homogenized in 1.15% KCL (1g/10ml solution). The mixture was centrifuged and the supernatant used for biochemical determinations in spectrophotometer.

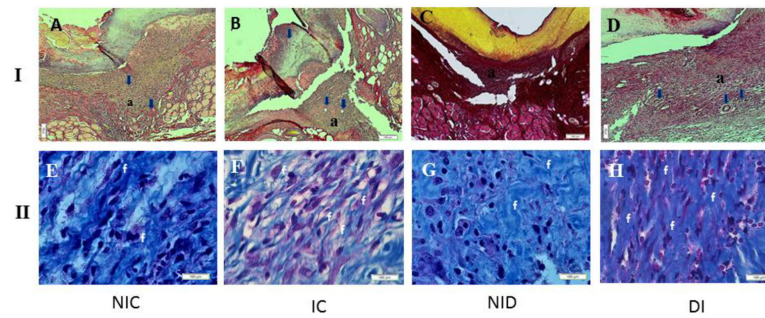


**Figure 3.**

I. Photomicrograph of experiment groups showing the differences about: granulation tissue

(**a**); newly formed blood vessels (**blue arrows**) and fibroblasts (**f**) (HE 10X). Figure 3.II.

Photomicrograph of experiment groups with Masson staining showing the differences about organization and collagen deposition (**c**). (20X)



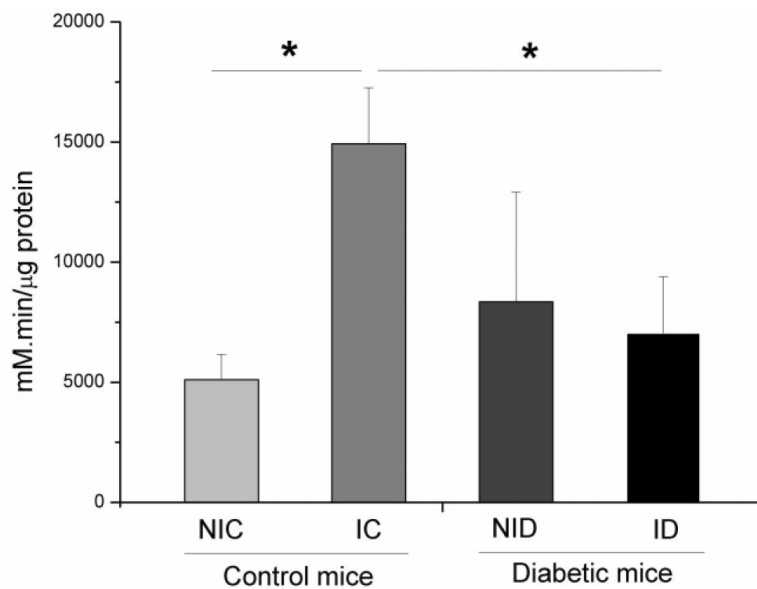


**Figure 4.** Catalase concentration levels in the skin of different groups: non-irradiated control (NIC), non-irradiated diabetic (NID), irradiated control (IC) and irradiated diabetic (ID). Infrared 904 nm laser irradiation was performed for 5 days consecutively after creation of the surgical lesion. ( $F = 11.028$ ,  $*p < 0.001$ ).

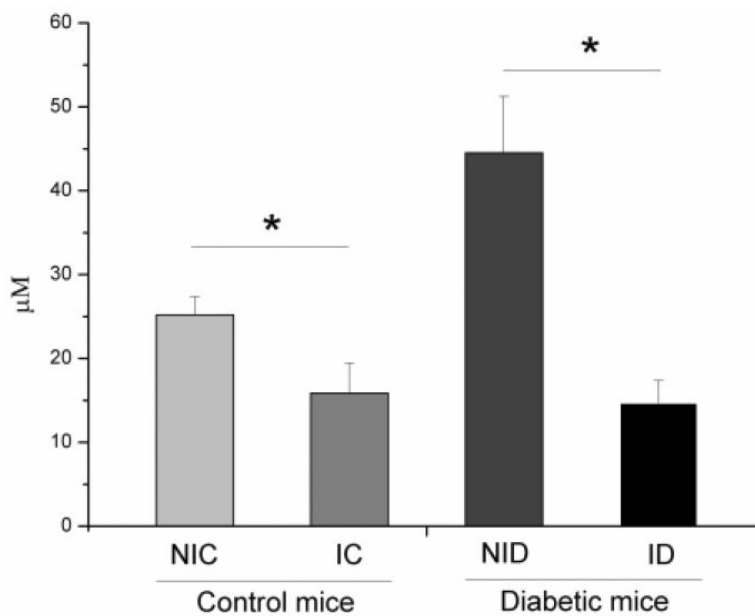


**Figure 5.** Nitrite concentration levels in the skin of different groups: non-irradiated control (NIC), non-irradiated diabetic (NID), irradiated control (IC) and irradiated diabetic (ID). Infrared 904 nm laser irradiation was performed for 5 days consecutively after creation of the surgical lesion. ( $F = 54.128$ ,  $p = 0.001$ ).

**Table 1**

## Laser Parameters

Irradiation and Treatment Parameters. The parameters were obtained at the IBRAMED (Brazil) for the AsGa laser, 904nm; model Laserpulse, handheld probe, used in contact to the mice skin.

Parameter [unit]	value
Center wavelength [nm]	904
Operating mode	pulsed
Frequency [Hz]	9500
Pulse duration [ns]	60
Duty cycle [%]	20
Energy per pulse [J]	42 nJ
Peak power [W]	70
Average power [mW]	39.9
Polarization	No
Spot size [cm <sup>2</sup> ]	0.1309
Beam shape	elliptical
Beam profile	Gaussian
Irradiance at target [mW/cm <sup>2</sup> ]	304.8
Exposure duration [sec]	60
Radiant exposure [J/cm <sup>2</sup> ]	18.288
Total Radiant energy [J]	2.394
Number of points irradiated	1
Area irradiated [cm <sup>2</sup> ]	0.1309
Application technique	Contact
Number and frequency of treatment sessions	1 × day / 5 days

**Table 2**

Statistical analysis using morphometric computational systems to determine amount collagen and angiogenesis analyzed by analysis of variance (ANOVA) one-way with Tukey post hoc test. The significance level was set at  $p < 0.05$ .

GROUPS	Collagen (Mean±SE)	Angiogenesis (Mean±SE)
<i>NIC<sup>(a)</sup></i>	3.82 ± 0.18 <sup>(b,d)</sup> *	10.18 ± 1.09
<i>IC<sup>(b)</sup></i>	4.99 ± 0.01	7.52 ± 1.32
<i>NID<sup>(c)</sup></i>	3.90 ± 0.01 <sup>(b,d)</sup> **	7.38 ± 0.99 <sup>(d)</sup> ***
<i>ID<sup>(d)</sup></i>	4.09 ± 0.01 <sup>(a,c)</sup> **	15.34 ± 1.14 <sup>(a,b,c)</sup> ***

\*  
p < 0.001;

\*\*  
p < 0.002;

\*\*\*  
p < 0.00

**Table 3**

TBARS concentration levels in the skin of different groups: non-irradiated control (NIC), non-irradiated diabetic (NID), irradiated control (IC) and irradiated diabetic (ID). The irradiation was performed by infrared 904nm laser for 5 days consecutively after the skin surgically lesion.

TBARS	n	Mean + DP	ANOVA
NIC	8	2.38 ± 0.29	
IC	8	5.05 ± 1.52*	
TBARS			0.001
NID	7	3.57 ± 1.37	
ID	7	1.65 ± 1.57*#	

\* P < 0.001 compared to each respective control group;

# relative to the group IC